Trans. of Korean Hydrogen and New Energy Society, Vol. 28, No. 2, 2017, pp. 137~143
DOI: https://doi.org/10.7316/KHNES.2017.28.2.137

KHNES
pISSN 1738-7264 • eISSN 2288-7407

수소 분위기에서 고 에너지 볼 밀링으로 제조한 80Mg+14Ni+6TaF_5합금의 수소와의 반응 속도와 수소 저장 용량

박혜령[1] · 송명엽[2†]

[1]전남대학교 화학공학부, [2]전북대학교 신소재공학부

Reaction Rate with Hydrogen and Hydrogen-storage Capacity of an 80Mg+14Ni+6TaF_5 Alloy Prepared by High-energy Ball Milling in Hydrogen

HYE RYOUNG PARK[1], MYOUNG YOUP SONG[2,†]

[1]School of Chemical Engineering, Chonnam National University, 77 Yongbong-ro, Buk-gu, Gwangju 61186, Korea
[2]Division of Advanced Materials Engineering, Hydrogen & Fuel Cell Research Center, Engineering Research Institute, Chonbuk National University, 567 Baekje-daero, Deokjin-gu, Jeonju 54896, Korea

[†]Corresponding author : songmy@jbnu.ac.kr

Received 25 January, 2017
Revised 17 February, 2017
Accepted 30 April, 2017

Abstract >> In the present study, Ni and TaF_5 were chosen as additives to enhance the hydriding and dehydriding rates of Mg. A sample with a composition of 80 wt% Mg + 14 wt% Ni + 6 wt% TaF_5 (named 80Mg+14Ni+6TaF_5) was prepared by high-energy ball milling in hydrogen. Its hydriding and dehydriding properties were then examined. At the fourth cycle, the activated sample absorbed 3.88 wt% H for 2.5 min, 4.74 wt% H for 5 min, and 5.75 wt% H for 60 min at 593 K under 12 bar H_2. 80Mg+14Ni+6TaF_5 had an effective hydrogen-storage capacity (the quantity of hydrogen absorbed for 60 min) of about 5.8 wt%. The sample desorbed 1.42 wt% H for 5 min, 3.42 wt% H for 15 min, and 5.09 wt% H for 60 min at 593 K under 1.0 bar H_2. Line scanning results by EDS for 80Mg+14Ni+6TaF_5 before and after cycling showed that the peaks of Ta and F appeared at different positions, indicating that the TaF_5 in 80Mg+14Ni+6TaF_5 was decomposed.

Key words : Hydrogen storage materials(수소 저장 재료), High-energy ball milling in hydrogen(수소 분위기에서 고 에너지 볼 밀링), Hydriding and dehydriding rates(수소 흡수 방출 속도), Scanning electron microscopy(주사 전자 현미경), Energy dispersive spectrometer(에너지 분산 형 분석기)

1. Introduction

Magnesium has many advantages as a hydrogen storage material[1-3]; a high hydrogen storage capacity (7.6 wt%), low cost, and abundance in the earth's crust[4]. However, its reaction rates with H_2 are very low.

Many works have been performed to increase the hydriding and dehydriding rates of magnesium[5-11].

In some works, magnesium hydride was employed as a starting material in order to increase the hydriding and dehydriding rates of magnesium by milling in a planetary mill with metal, compound, or oxide[12-14]. In this work, we used Mg instead of MgH_2 as one of the starting materials.

Ni-added Mg alloys[5,6] and mechanically-alloyed Mg with Ni under an Ar atmosphere[15-18] had the increased hydriding and dehydriding rates of Mg. According to Bobet et al.[19], the hydrogen storage properties of pure Mg and10 wt% Co, Ni, or Fe-Mg mixtures were improved by milling in planetary ball mill under H_2 for a relatively short time of 2 h.

Malka et al.[20] investigated the effects of added chlorides and fluorides of various metals on the dehydriding temperature of MgH_2. They reported that among the halides studied, ZrF_4, TaF_5, NbF_5, VCl_3, and $TiCl_3$ showed the best catalysts for the decomposition of MgH_2.

The magnesium-based samples prepared by high-energy ball milling in hydrogen with transition elements or oxides had relatively high hydriding and dehydriding rates when about 20% was added.

In the present work, Ni as an element and TaF_5 as a halide were chosen to add to Mg in order to enhance the hydriding and dehydriding rates. A sample with a composition of 80 wt% Mg + 14 wt% Ni + 6 wt% TaF_5, which contained additives of 20 wt%, was prepared by high-energy ball milling in hydrogen. The hydriding and dehydriding properties of the sample were then investigated. We named 80 wt% Mg + 14 wt% Ni + 6 wt% TaF_5 as 80Mg+14Ni+6TaF_5.

2. Experimental details

Pure Mg powder (particle size 74-149 μm, purity 99.6%, Alfa Aesar), Ni powder (average particle size 2.2 ~ 3.0 μm, purity 99.9% metal basis, C typically < 0.1%, Alfa Aesar), and TaF_5 (Tantalum (V) fluoride, purity 98%, Aldrich) were used as starting materials.

High-energy ball milling in hydrogen was carried out in a planetary ball mill (Planetary Mono Mill; Pulverisette 6, Fritsch). The total weight of the mixture with the planned composition was 8 g and that of 105 hardened steel balls was 360 g. The mixture and the steel balls were mixed in a hermetically sealed stainless steel container (with a volume of 250 mL) with a disc revolution speed of 250 rpm. The sample was handled in an Ar-filled glove box. The pressure of high purity hydrogen gas in the mill container was about 12 bar. Milling time was 6 h by repeating milling for 15 min and resting 5 min. The hydrogen absorbed by the mixture during milling was made up by refilling hydrogen every two hours.

A Sieverts' type hydriding and dehydriding apparatus, described previously[21], was used to measure the absorbed or desorbed hydrogen quantity as the reaction progresses. A used amount of the samples was 0.5 g for these measurements. After the absorbed and then desorbed hydrogen quantities were measured at desired temperatures for 1 h under 12 and 1.0 bar H_2, respectively, the samples were vacuum-pumped at 623 K for 2 h. The micrographs of the samples were obtained using a JSM-6400 scanning electron microscope (SEM) operated at 20 kV. The elements in the particles of the samples after milling and after hydriding-dehydriding cycling were analyzed by line scanning with an energy dispersive spectrometer (EDS, EDAX).

3. Results and discussion

The weight percentages of absorbed hydrogen, H_a, and desorbed hydrogen, H_d, are expressed with re-

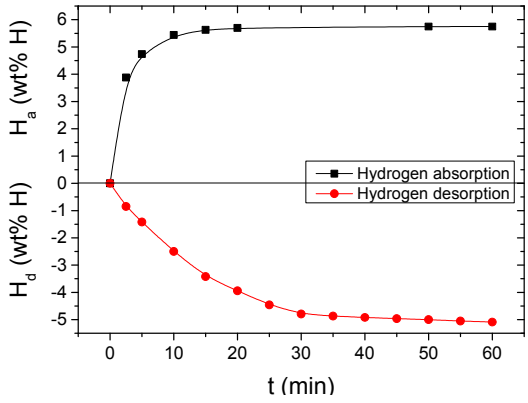

Fig. 1. H_a versus t curve under 12 bar H_2 and H_d versus t curve under 1.0 bar H_2 at 593 K at n=4 for 80Mg+14Ni+6TaF_5

Table 1. Variations of H_a under 12 bar H_2 and H_d under 1.0 bar H_2 with time at 593 K at n=4 for 80Mg+14Ni+6TaF_5

	2.5 min	5 min	10 min	15 min	30 min	60 min
H_a	3.88	4.74	5.44	5.63	5.71	5.75
H_d	0.85	1.42	2.50	3.42	4.79	5.09

spect to sample weight. Fig. 1 shows the H_a vs. t curve under 12 bar H_2 and H_d vs. t curve under 1.0 bar H_2 at 593 K at n=4 for 80Mg+14Ni+6TaF_5. The initial hydriding rate is quite high and the sample absorbs 3.88 wt% H for 2.5 min, 4.74 wt% H for 5 min, 5.44 wt% H for 10 min, and 5.75 wt% H for 60 min. The effective hydrogen-storage capacity is defined as the quantity of hydrogen absorbed for 60 min. 80Mg+14Ni+6TaF_5 has an effective hydrogen-storage capacity of about 5.8 wt%. The initial dehydriding rate is low, compared with the initial hydriding rate, and the sample desorbs 0.85 wt% H for 2.5 min, 1.42 wt% H for 5 min, 3.42 wt% H for 15 min, and 5.09 wt% H for 60 min. Table 1 presents the variations of H_a under 12 bar H_2 and H_d under 1.0 bar H_2 with time at 593 K at n=4 for 80Mg+14Ni+6TaF_5.

The hydriding and dehydriding rates are expressed as dH_a/dt and dH_d/dt, respectively, where t is time. The variations of the hydriding rate, dH_a/dt, under 12 bar H_2 and the dehydriding rate, dH_d/dt, under 1.0 bar H_2 with time at 593 K for activated 80Mg+14Ni+6TaF_5

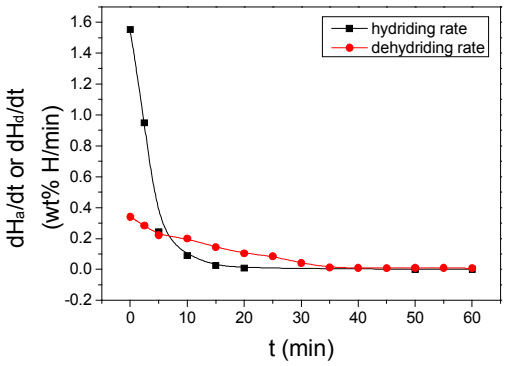

Fig. 2. Variations of the hydriding rate, dH_a/dt, under 12 bar H_2 and dehydriding rate, dH_d/dt, under 1.0 bar H_2 with time at 593 K for activated 80Mg+14Ni+6TaF_5 (at n=4)

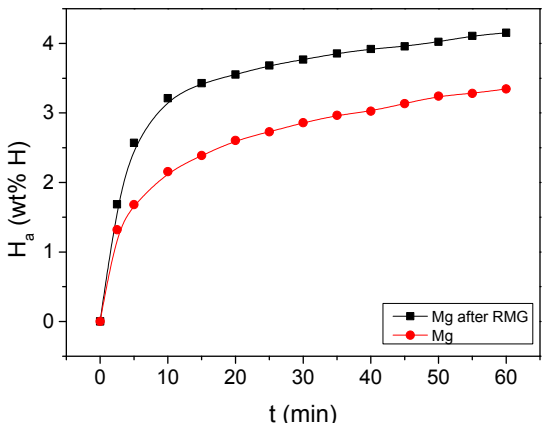

Fig. 3. H_a versus t curves at 593 K under 12 bar H_2 at n=7 for Mg and Mg after RMG at n=7

(at n=4) are shown in Fig. 2. The hydriding rate decreases very rapidly in the beginning and become almost zero after about 15 min. The dehydriding rate decreases gradually in the beginning and become almost zero after about 35 min. The hydriding and dehydriding reactions progress by the nucleation and growth mechanism which exhibits two stages of the nucleation-growth stage and growth-impingement stage. Fig. 2 shows that the dH_a/dt vs. t and dH_d/dt vs. t curves exhibit only the later stage, the growth-impingement stage. This indicates that the addition of Ni and TaF_5 by high-energy ball milling in hydrogen facilitates the nucleation of the magnesium hydride

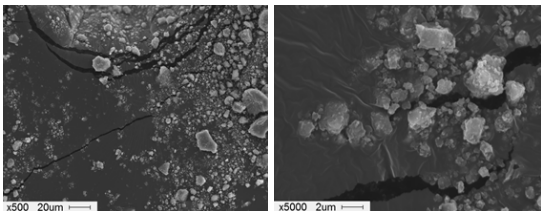

Fig. 4. SEM micrographs of 80Mg+14Ni+6TaF_5 after high-energy ball milling in hydrogen

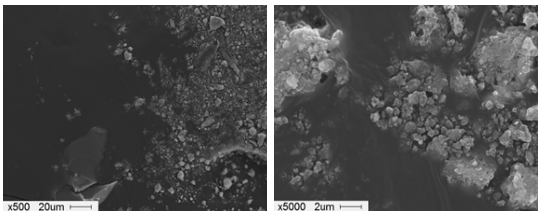

Fig. 5. SEM micrographs of 80Mg+14Ni+6TaF_5 after hydriding-dehydriding cycling (n=4)

in the hydriding reaction and the nucleation of the solid solution of magnesium with hydrogen in the dehydriding reaction, making the nucleation-growth stage disappear.

Fig. 3 shows the H_a versus t curves at 593 K under 12 bar H_2 for Mg and Mg after RMG at n=7. High-energy ball milling in hydrogen is called reactive mechanical grinding (RMG). At n=7, Mg after RMG has a higher initial hydrogenation rate and a larger quantity of hydrogen absorbed for 60 min than Mg. Mg absorbs 1.68 wt% H for 5 min, 2.16 wt% H for 10 min, 2.86 wt% H for 30 min, and 3.35 wt% H for 60 min. Mg after RMG absorbs 2.57 wt% H for 5 min, 3.21 wt% H for 10 min, 3.77 wt% H for 30 min, and 4.15 wt% H for 60 min. Comparison of Fig. 1 and Fig. 3 indicates that 80Mg+4Ni+6TaF_5 has a much higher initial hydriding rate and a much larger effective hydrogen-storage capacity than Mg and Mg after RMG.

Fig. 4 shows the SEM micrographs of 80Mg+14Ni+ 6TaF_5 after high-energy ball milling in hydrogen. The sample after high-energy ball milling in hydrogen has small and large particles. The particle sizes are not homogeneous. The large particles have flat surfaces.

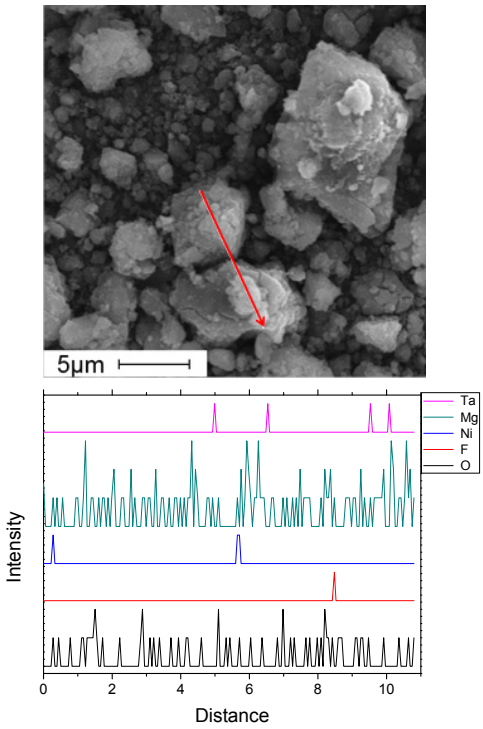

Fig. 6. BSE (back-scattered electrons) images and line scanning results by EDS for 80Mg+14Ni+6TaF_5 after high-energy ball milling in hydrogen

The SEM micrographs of 80Mg+14Ni+6TaF_5 after hydriding-dehydriding cycling at 593 K (n=4) are shown in Fig. 5. The sample after hydriding-dehydriding cycling also has small and large particles. The particles are smaller than those of the sample after high-energy ball milling in hydrogen. Expansion of particles occurs during hydriding reaction and contraction of particles occurs during dehydriding reaction. Repetition of expansion and contraction of particles is believed to lead to the decrease in the particle size.

Fig. 6 shows the BSE (back-scattered electrons) images and line scanning results by EDS for 80Mg+14Ni+6TaF_5 after high-energy ball milling in hydrogen. The particle sizes are not homogeneous. The large

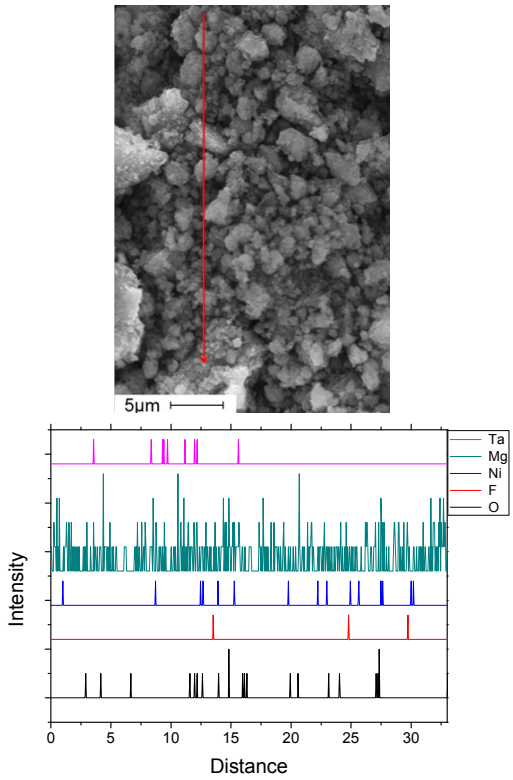

Fig. 7. BSE (back-scattered electrons) images and line scanning results by EDS for 80Mg+14Ni+6TaF_5 after hydriding-dehydriding cycling (n=4)

particles have flat surfaces. Fine particles are observed on the large particles. The composition along the scanned line for the sample after high-energy ball milling in hydrogen is 31.44 wt% O, 0.54 wt% F, 1.63 wt% Ni, 64.23 wt% Mg, and 2.17 wt% Ta. Excluding oxygen, the composition becomes approximately 94 wt% Mg + 2 wt% Ni + 4 wt% (Ta+F), which is quite different from the composition of the sample of 80 wt% Mg + 14 wt% Ni + 6 wt% TaF_5. Peaks of Ta and F appear at different positions, showing that TaF_5 was decomposed after reactive mechanical grinding. The peak of F appears at the position where the peak of Mg appears, suggesting that an Mg-F compound may have formed. It is reported that MgF_2 forms in TaF_5-containing Mg alloys after high-energy ball milling in hydrogen[22-24].

The BSE (back-scattered electrons) images and line scanning results by EDS for 80Mg+14Ni+6TaF_5 after hydriding-dehydriding cycling (n=4) are shown in Fig. 7. Particles and agglomerates after hydriding-dehydriding cycling are smaller than those after high-energy ball milling in hydrogen. The composition along the scanned line for the sample after hydriding-dehydriding cycling (n=4) is 5.18 wt% O, 0.71 wt% F, 3.53 wt% Ni, 88.46 wt% Mg, and 2.12 wt% Ta. Peaks of Ta and F appear at different positions, showing that TaF_5 was decomposed after reactive mechanical grinding. The peak of F appears at the position where the peak of Mg appears, suggesting that an Mg-F compound may have formed. It is reported that MgF_2 forms in TaF_5–containing Mg alloys after hydriding-dehydriding cycling[22-24]. Yavari et al[25]. obtained powders with highly increased hydriding and dehydriding kinetics at 573 K by adding transition metal fluorides such as FeF_3 to MgH_2. They reported that a fluorine transfer reaction produced protective MgF_2 and Fe nanoparticles, which could act as a catalyst.

The addition of Ni and TaF_5 to Mg by high-energy ball milling in hydrogen is considered to create defects on the surface and inside of Mg, to produce clean surfaces, and to reduce the particle size of Mg. These phenomena increase nucleation rate, the reactivity of particle surfaces, and the diffusion rate of hydrogen atoms, respectively. Fig. 2 shows that the addition of Ni and TaF_5 by reactive mechanical grinding enhances the nucleation of the magnesium hydride and the solid solution of magnesium with hydrogen.

The XRD pattern of 80Mg+14Ni+6TaF_5 after high-energy ball milling in hydrogen revealed the presence of Ni, Mg, β-MgH_2, γ-MgH_2, MgF_2, and Ta_2H in the sample. The XRD pattern of 80Mg+4Ni+6TaF_5 dehydrided at the 4th hydriding-dehydrid-

ing cycle showed the inclusion of Mg, Mg_2Ni, β-MgH_2, and small amounts of MgO, MgF_2, and Ta_2H in the sample.

Mg_2Ni has higher hydriding and dehydriding rates than Mg. The formation of Mg_2Ni phase with the reaction of Ni with Mg during hydriding-dehydriding cycling makes higher the hydriding rate of Mg and the dehydriding rate of MgH_2. It is considered that β-MgH_2, γ-MgH_2, MgF_2, and Ta_2H formed during high-energy ball milling in hydrogen help the particles pulverized more effectively. Jin et al.[26] reported that in the transition metal fluorides-added MgH_2, the hydriding kinetics of MgH_2 is improved by a role of the hydride phases formed during milling and/or hydriding reaction.

4. Conclusions

A sample with a composition of 80 wt% Mg + 14 wt% Ni + 6 wt% TaF_5 (named 80Mg+14Ni+6TaF_5) was prepared by high-energy ball milling in hydrogen. At the fourth cycle, the activated sample absorbed 3.88 wt% H for 2.5 min, 4.74 wt% H for 5 min, and 5.75wt% H for 60 min at 593 K under 12 bar H_2. 80Mg+14Ni+6TaF_5 had an effective hydrogen-storage capacity (the quantity of hydrogen absorbed for 60 min) of about 5.8 wt%. The sample desorbed 1.42 wt% H for 5 min, 3.42 wt% H for 15 min, and 5.09 wt% H for 60 min at 593 K under 1.0 bar H_2. The addition of Ni and TaF_5 by high-energy ball milling in hydrogen and hydriding-dehydriding cycling is believed to create defects on the surface and inside of Mg, to produce clean surfaces, and to reduce the particle size of Mg. Line scanning results by EDS for 80Mg+14Ni+6TaF_5 before and after cycling showed that the peaks of Ta and F appeared at different positions, indicating that TaF_5 was decomposed.

References

1. S.H. Lee, H.R. Park, M.Y. Song, “Change in Hydrogen-Storage Performance of Transition Metals and $NaAlH_4$-Added MgH_2 with Thermal and Hydriding-Dehydriding Cycling”, Korean J. Met. Mater., Vol. 53, No. 2, 2015, p. 133.
2. S.H. Lee, Y.J. Kwak, H.R. Park, M.Y. Song, “Enhancement of the Hydriding and Dehydriding Rates of Mg by Adding $TiCl_3$ and Reactive Mechanical Grinding”, Korean J. Met. Mater., Vol. 53, No. 3, 2015, p. 187.
3. Y.J. Kwak, S.N. Kwon, S.H. Lee, I.W. Park, M.Y. Song, “Synthesis of $Zn(BH_4)_2$ and Gas Absorption and Release Characteristics of $Zn(BH_4)_2$, Ni, or Ti-Added MgH_2–Based Alloys”, Korean J. Met. Mater., Vol. 53, No. 7, 2015, p. 500.
4. D.R. Mumm, S.H. Lee, M.Y. Song, “Cycling Behavior of Transition Metals and Sodium Alanate-Added MgH_2 Kept in a Glove Box”, Korean J. Met. Mater., Vol. 53, No. 8, 2015, p. 584.
5. J.J. Reilly and R.H. Wiswall Jr, “The Reaction of Hydrogen with Alloys of Magnesium and Nickel and the Formation of Mg_2NiH_4”, Inorg. Chem., Vol. 7, No. 11, 1968, p. 2254.
6. E. Akiba, K. Nomura, S. Ono and S. Suda, “Kinetics of the Reaction between Mg-Ni Alloys and H_2”, Int. J. Hydrogen Energy, Vol. 7, No. 10, 1982, p. 787.
7. Y.J. Kwak, S.N. Kwon, M.Y. Song, “Hydriding and Dehydriding Properties of Zinc Borohydride, Nickel, and Titanium-Added Magnesium Hydride”, Korean J. Met. Mater., Vol. 53, No. 11, 2015, p. 808.
8. S.H. Hong, M.Y. Song, “MgH_2 and Ni-Coated Carbon-Added Mg Hydrogen-Storage Alloy Prepared by Mechanical Alloying”, Korean J. Met. Mater., Vol. 54, No. 2, 2016, p. 125.
9. M.Y. Song, Y.J. Kwak, S.H. Lee, H.R. Park, “Enhancement of Hydrogen Storage Characteristics of Mg by Addition of Nickel and Niobium (V) Fluoride via Mechanical Alloying”, Korean J. Met. Mater., Vol. 54, No. 3, 2016, p. 210.
10. M.Y. Song, Y.J. Kwak, H.R. Park, “Hydrogen Storage Characteristics of Metal Hydro-Borate and Transition Element-Added Magnesium Hydride”, Korean J. Met. Mater., Vol. 54, No. 7, 2016, p. 503.
11. S.N. Kwon, H.R. Park, M.Y. Song, “Hydrogen Storage and Release Properties of Transition Metal-Added Magnesium Hydride Alloy Fabricated by Grinding in a Hydrogen Atmosphere”, Korean J. Met. Mater., Vol. 54, No. 7, 2016, p. 510.
12. W. Oelerich, T. Klassen, R. Bormann, “Comparison of the Catalytic Effects of V, V_2O_5, VN, and VC on the Hydrogen Sorption of Nanocrystalline Mg”, J. Alloy Compd., Vol. 322, No. 1-2, 2001, p. L5.

13. Z. Dehouche, T. Klassen, W. Oelerich, J. Goyette, T. K. Bose, R. Schulz, "Cycling and Thermal Stability of Nano-structured MgH_2-Cr_2O_3 Composite for Hydrogen Storage", J. Alloy Compd., Vol. 347, 2002, p. 319.
14. G. Barkhordarian, T. Klassen, R. Bormann, "Fast Hydrogen Sorption Kinetics of Nanocrystalline Mg Using Nb_2O_5 as Catalyst", Scripta Materialia, Vol. 49, No. 3, 2003, p. 213.
15. M. Y. Song, "Improvement in Hydrogen Storage Characteristics of Magnesium by Mechanical Alloying with Nickel", J. Mater. Sci., Vol. 30, 1995, p. 1343.
16. M.Y. Song, E.I. Ivanov, B. Darriet, M. Pezat, P. Hagenmuller, "Hydriding Properties of a Mechanically Alloyed Mixture with a Composition Mg_2Ni", Int. J. Hydrogen Energy, Vol. 10, No. 3, 1985, p. 169.
17. M.Y. Song, E.I. Ivanov, B. Darriet, M. Pezat, P. Hagenmuller, "Hydriding and Dehydriding Characteristics of Mechanically Alloyed Mixtures Mg-xwt.%Ni (x=5, 10, 25 and 55)", J. Less-Common Met., Vol. 131, 1987, p. 71.
18. M.Y. Song, "Effects of Mechanical Alloying on the Hydrogen Storage Characteristics of Mg-x wt.%Ni (x=0, 5, 10, 25 and 55) Mixtures", Int. J. Hydrogen Energy, Vol. 20, No. 3, 1995, p. 221.
19. J.-L. Bobet, E. Akiba, Y. Nakamura, B. Darriet,. "Study of Mg-M (M=Co, Ni and Fe) Mixture Elaborated by Reactive Mechanical Alloying - Hydrogen Sorption Properties", Int. J. Hydrogen Energy, Vol. 25, 2000, p. 987.
20. I.E. Malka, T. Czujko, J. Bystrzycki, "Catalytic Effect of Halide Additives Ball Milled with Magnesium Hydride", Int. J. Hydrogen Energy, Vol. 35, No. 4, 2010, p. 1706.
21. M.Y. Song, S.H. Baek, J.-L. Bobet, S.H. Hong, "Hydrogen Storage Properties of a Mg-Ni-Fe Mixture Prepared via Planetary Ball Milling in a H_2 Atmosphere", Int. J. Hydrogen Energy, Vol. 35, 2010, p. 10366.
22. M.Y. Song, Y.J. Kwak, S.H. Lee, H.R. Park, "Development of Mg-14Ni-6TaF_5 Hydrogen Storage Material via Reactive Mechanical Grinding", Mater. Sci., Vol. 4, 2014, p. 440.
23. M.Y. Song, Y.J. Kwak, S.H. Lee, H.R. Park, "Enhancement of Reaction Kinetics with Hydrogen of Mg by Addition of Ni and TaF_5 via Reactive Mechanical Grinding", Korean J. Met. Mater., Vol. 51, No. 1, 2013, p. 51.
24. D.R. Mumm, Y.J. Kwak, H.R. Park, M.Y. Song, "Effects of Milling and Hydriding-Dehydriding Cycling on the Hydrogen-Storage Behaviors of a Magnesium-Nickel-Tantalum Fluoride Alloy", Korean J. Met. Mater., Vol.53, No. 12, 2015, p. 904.
25. A.R. Yavari, A. LeMoulec, F.R. de Castro, S. Deledda, O. Friedrichs, W.J. Botta, G. Vaughan, T. Klassen, A. Fernandez, A. Kvick, "Improvement in H-Sorption Kinetics of MgH_2 Powders by Using Fe Nanoparticles Generated by Reactive FeF_3 Addition", Scripta Materialia, Vol. 52, No. 8, 2005, p. 719.
26. S.-A. Jin, J.-P. Ahn, J.-H. Shim, Y.W. Cho, K.-W. Yi, "Dehydrogenation and Hydrogenation Characteristics of MgH_2 with Transition Metal Fluorides", J. Power Sources, Vol. 172, 2007, p. 859.